Received: 12 February 2021 | Revised: 2 February 2022 | Accepted: 7 March 2022

DOI: 10.1111/fog.12582

ORIGINAL ARTICLE

FISHERIES OCEANOGRAPHY WILEY

Where do recruits come from? Backward Lagrangian simulation for the deep water rose shrimps in the Central Mediterranean Sea

Francesco Gargano[1] | Germana Garofalo[2] | Federico Quattrocchi[2] | Fabio Fiorentino[2]

[1]Department of Engineering, University of Palermo, Palermo, Italy

[2]National Research Council-Institute for Marine Biological Resources and Biotechnology (CNR IRBIM), Mazara del Vallo, Italy

Correspondence
Germana Garofalo, National Research Council-Institute for Marine Biological Resources and Biotechnology (CNR IRBIM), SS Mazara del Vallo, Via L. Vaccara 61, 91026, Mazara del Vallo (TP), Italy.
Email: germana.garofalo@cnr.it

Funding information
European Commission-Directorate General MARE (Maritime Affairs and Fisheries)

Abstract

Backward-in-time Lagrangian dispersion models can efficiently reconstruct drifters trajectories by linking known arrival positions to potential sources. This approach was applied to the deep water rose shrimp (*Parapenaeus longirostris*) in the Strait of Sicily (central Mediterranean Sea). The objective was to identify the potential spawning areas of the larvae that settle in the known nursery grounds of the northern sector of the Strait of Sicily, thus quantifying the extent of the potential contribution to recruitment from the surrounding regions. Numerical simulations were performed over 11 years (2005–2015) and for two different periods (spring/summer and autumn/winter) corresponding to the species' spawning peaks in the region. The persistence over time of potential spawning areas was identified through a Hotspot analysis of the backward trajectories end-points, filtered to meet a suitable depth range for spawners. The results confirmed the expected downstream connectivity between spawning and nursery grounds along the Sicilian–Maltese shelf and, notably, indicated that these spawning grounds contribute to the high productivity and resilience of deep water rose shrimp fisheries in the northern Strait of Sicily more than the spawning grounds in surrounding regions. A minor and time-varying contribution is due to potential spawning areas identified on the African shelf. These results are important to adequately define the geographical scale for the assessment and management of this important fishery resource in the Strait of Sicily. In particular, the assumption of a single stock that does not consider the spatial structure of the population should be revised for the purpose of fisheries management.

KEYWORDS
connectivity, hotspot analysis, larval transport, *Parapenaeus longirostris*, stock structure

1 | INTRODUCTION

Fish recruitment dynamics is a critical topic in fishery science because its understanding plays a major role in fisheries management. Recruits, expressed as any group of young fish joining a population, are normally assumed to derive from a reproductively distinct, self-sustaining population called classically "stock unit." This implies that demography of population inhabiting a given area reflects recruitment due to the local spawning stock rather than arrival of eggs/larvae from adjacent areas. Fish mortality after recruitment is also entirely due to internal processes (fishery removals, predation, etc.), thus excluding immigration and/or emigration to other areas (Cadrin et al., 2019; Hilborn et al., 2003).

The spawning stock recruitment relationships, linking the parental stock size of a population to subsequent recruitment, are among the most complex issues in the dynamics of exploited resources. These relationships are affected by density (compensatory mortality) and non-density (e.g., environmental) dependent factors regulating recruits survival (Cury et al., 2014; Levi et al., 2003; Ottersen et al., 2013; Patti et al., 2020).

In the last decades the classical vision of the stock unit as an isolated population has been questioned and a more complex spatial structure of exploited stocks has been proposed, which assumes the existence of various population subunits and significant exchanges of individuals between them (Ciannelli et al., 2013; Kritzer & Liu, 2014). Based on this new paradigm, resolving the mismatch between biological stock and management units is recognized as critical for the reliable assessment and management of fishery resources (Kerr et al., 2017). Indeed, ignoring population spatial structure and related connectivity among population subunits can affect the accurate description of stock dynamics due to the misperception of the processes that support their persistence (Cadrin, 2020). A recent work by Hidalgo et al. (2019) provided evidence that larval connectivity between hake subpopulations in three contiguous management units in the western Mediterranean was able to explain a fraction of interannual variability of the species recruitment in each unit larger than that explained by spawning stock biomass alone. In other words, identifying the self-sustaining populations requires to know the space–time patterns of larval dispersal connecting spawning areas to nurseries, and migrations of juveniles and adults toward the feeding and spawning areas. We have shown in Figure 1 a non-exhaustive scheme of the possible exchanges between spawning and nursery grounds in contiguous areas. The figure highlights how, for the purposes of stock assessment, it is essential to understand which parental stock is producing recruitment within a given area.

However, spatially-explicit data covering different vital phases are not easily obtained and simulation is considered as a useful approach to investigate the spatial structure of populations (Cadrin et al., 2019; Kerr & Goethel, 2014; Werner et al., 2007).

In the last decade, plenty of such simulation exercises have been conducted in the Mediterranean Sea and, in particular, in the Strait of Sicily (SoS hereafter) where Lagrangian transport models have been developed to investigate the dispersal of early life stages (eggs/larvae) of both pelagic and demersal species (Falcini et al., 2015; Falcini et al., 2020; Gargano et al., 2017; Palatella et al., 2014; Patti et al., 2020; Quattrocchi et al., 2019; Torri et al., 2018).

Among these, we mention the work by Quattrocchi et al. (2019) who studied the connectivity between spawning and nursery areas of the high commercial value deep water rose shrimp, *P. longirostris* (Lucas, 1846; hereafter DPS, according to the FAO 3alphacode for the species) by applying a forward Lagrangian model. The model outcomes displayed a connectivity between spawning and nursery areas in the north side of the SoS, with long-distance connections modulated by the decadal variation in the hydrodynamic regime. Expanding the area of investigation southward, a weak connectivity between spawning grounds in the northern SoS and nurseries on the African outer shelf was observed. In short, the work by Quattrocchi et al. (2019) contributed to answer the question of what the fate of the eggs/larvae released in the known spawning areas of the northern SoS is.

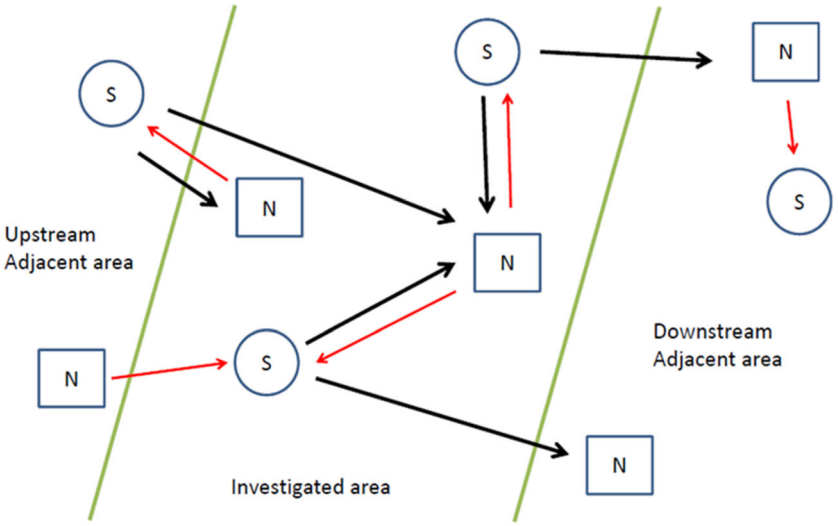

FIGURE 1 Schematized representation of possible connectivity patterns between spawning and nursery grounds in adjacent areas, linked by larval dispersal (black arrows) and spawning migrations (red arrows). N and S indicate the nursery and spawning areas respectively. Migrations from N or S to feeding areas are not considered. A main objective for stock assessment is to understand what is the parental stock producing recruitment inside a management unit (investigated area between green lines)

The objective of our study is to shed more light on the fundamental issue of DPS recruitment dynamics and stock structure in the SoS by reversing the question, that is, where the eggs/larvae that settle on the known nursery areas of the northern SoS have been originated. In recent years, several authors have applied larval dispersal models in backtracking mode to identify the potential spawning grounds of a range of species, including coastal fish (Calò et al., 2018; Legrand et al., 2019; Torrado et al., 2021), small pelagics (European anchovy; Falcini et al., 2020) and deep-sea demersal species such as the Blue and red shrimp *Aristeus antennatus* (Clavel-Henry et al., 2021). Our interest for the DPS is due to its high commercial importance for the trawl fisheries in the SoS with an estimated annual yield ranging from 7000 and 10,000 tons in the last years (FAO-GFCM, 2019). The exploitation of this stock is shared between Italian, Tunisian and Maltese bottom trawlers and it has recently been assessed in overfishing status within the framework of the General Fisheries Commission for the Mediterranean Sea (GFCM) (FAO-GFCM, 2019). Since 2015 an international multiannual management plan was adopted by the GFCM (Recommendation GFCM/42/2018/5, FAO-GFCM, 2019). Due to the poor knowledge of its geographical structure, the DPS stock is managed as a straddling stock distributed in the five GFCM Geographical subunits (GSAs) in which the SoS is divided (GSA 12, 13, 14, 15 and 16).

In this context, we applied a backward-in-time Lagrangian dispersion model (1) to assess the extent to which potential spawning areas in the central Mediterranean feed the nurseries located in the northern SoS (Sicilian–Maltese shelf); (2) to quantify the time persistence of the potential spawning areas; (3) to extend our knowledge of larval connectivity between management units in the SoS in order to delineate self-sustaining units and justify unit-stock assumptions in stock assessment models (Cadrin et al., 2019).

2 | MATERIALS AND METHODS

2.1 | The environmental characteristics of the study area

The SoS connects the western and eastern Mediterranean and is characterized by a complex bottom topography, including two wide and shallow banks in the north along the western (Adventure Bank) and eastern (Malta Bank) sectors of the Sicilian coast, and a shallow continental platform (less than 30-m depth) in the south extending for more than 100 nautical miles from the Tunisian coast (Garofalo et al., 2018). The slope between Sicily and Malta is incised by deep trenches and steep slopes while it is very gentle between Malta and Libya. The circulation is mainly controlled by the Modified Atlantic Water flowing eastward in the upper layer, and the Levantine intermediate Water flowing westward mainly in the 200–500 m depth range. Entering the SoS, the Atlantic Water bifurcates into the Atlantic Ionian Stream (AIS) along the south Sicilian coast and the Atlantic Tunisian Current (ATC) along the Tunisian shelf (Béranger et al., 2004), both characterized by significant annual and seasonal variability (Sorgente et al., 2003). The AIS generally has a stronger circulation over the ATC during the spring/summer season, and despite the annual variability, exhibits some persistent hydrographic features. Along its meandering path on the Sicilian platform, the AIS circulates around two large semi-permanent cyclonic vortices, the first one lying over the Adventure Bank and the second over the Malta shelf, and this favors the existence of upwelling phenomena (Piccioni et al., 1988). Decadal changes in the surface sea current system of the SoS were recently described and related to the overall circulation changes in the Ionian Sea, namely the periodic reversal between cyclonic and anticyclonic regime (Northern Ionian Reversal phenomenon; Pinardi et al., 2015). The driving force of this phenomenon is still debated in the scientific community and several mechanisms have been proposed to explain this phenomenon, mostly related to the wind stress curl changes (Pinardi et al., 2015), and the salinity gradients originated from the various water masses flowing into the Ionian Sea, a condition known as the Adriatic-Ionian Bimodal Oscillation System BiOS, (see Crisiani & Mosetti, 2016; Gačić et al., 2010). More important, the AIS strength seems strongly correlated to this reversal phenomenon. In the period of high intensity of the AIS, surface water flows from the SoS into the northern part of the Ionian Sea producing an overall anticyclonic circulation; conversely, when the AIS is weak, water flows into the Ionian Sea at the latitude of around 36°N, supporting a cyclonic circulation. In particular, considering the time period 2005–2015, 2005 is the last year of a cyclonic regime, the anticyclonic regime covers the years 2006–2010, and surprisingly 2011 and 2012 still alternate the cyclonic and anticyclonic regime (Gačić et al., 2014). At the beginning of 2013 the cyclonic regime is restored (Liu et al., 2021). Overall, rather variable regimes of AIS intensity have characterized the decade 2005–2015.

2.2 | The life cycle of the deep-water rose shrimp

Deep water rose shrimp is an epi-benthic species widely distributed in the Eastern Atlantic Ocean and in the whole Mediterranean Sea (Sobrino et al., 2005). It is observed in all seas surrounding Italy, predominantly in the Ionian Sea and the SoS (Abellò et al., 2002; Sobrino et al., 2005), at depths between 20 and 750 m depth although the highest abundances are found between 100 and 400 m (Fortibuoni et al., 2010; Politou et al., 2008). The species shows a marked size-related bathymetric distribution linked to ontogenetic migrations, being larger individuals found at greater depths compared to small and medium size individuals (Fortibuoni et al., 2010; Politou et al., 2008).

Adults are mainly distributed in the upper slope, 200- to 400-m depth (Politou et al., 2008) but Dos Santos (1998) suggested that, during the spawning season, they move to shallower waters (around the 100 m isobath) to reproduce. According to Fortibuoni et al. (2010) mature females are mainly found at bottoms between 150 and 350 m deep in the northern SoS, where the authors found three main persistent spawning grounds, respectively on the eastern and western edge of the Adventure Bank and east of the Malta Bank.

Although mature females are present throughout the year (De Ranieri et al., 1998; Levi et al., 1995), suggesting that the species has an extended spawning activity, one-to-three peaks in spring/summer and autumn/winter have been observed across the Mediterranean, depending on location, water temperature and females' size (Bianchini et al., 2010, and references therein).

Scarce information is available on eggs and larvae of the species, which are usually found in low abundances in zooplankton samples (Pires et al., 2021). Dos Santos (1998) observed high densities of DPS larvae in the water column around 100 m depth, while Torres et al. (2013) reported that larvae of DPS were captured in surface waters over the shelf break off the Balearic Islands. Larvae could have vertical migrations (Dos Santos et al., 2008) that impact their spatial distribution, and consequently the dispersal and connectivity patterns (Pires et al., 2021). Even less is known about the duration of the dispersion phase. The development of the larval phase lasts from 30 days (Pires et al., 2021) to at least 2 months (Heldt, 1938). Recruits (<20-mm carapace length) are generally found within 200-m depth (Fortibuoni et al., 2010; Politou et al., 2008). In the northern SoS, the presence of nursery grounds, that is, areas with high densities of recruits and great spatio-temporal stability, was first established by Fortibuoni et al. (2010) using data from experimental trawl surveys, and further documented by Garofalo et al. (2011) and Colloca et al. (2015). They are mostly located on muddy bottoms of the outer shelf (up to 200 m) and are highly persistent in time. Figure 2 shows the location of the persistent nursery grounds (Colloca et al., 2015) considered in the present study.

2.3 | The Lagrangian model

We simulated larval transport using the Lagrangian model already introduced and applied for standard forward-in-time simulations in the SoS (Gargano et al., 2017; Palatella et al., 2014; Quattrocchi et al., 2019). In the present work, we applied the model with backward-in-time simulations.

This model arises under the main hypothesis that eggs and larvae are particles passively subjected to hydrographic forcing in surface waters. The transport is governed by a 3D marine velocity field which is given by the superposition of a large scale velocity field and a small scale turbulent field which reproduces the chaotic behavior of the marine currents.

The main 3D large-scale marine current velocity fields during the DPS spawning period were obtained from the Mediterranean Sea Forecasting System (hereafter MFS; Tonani et al., 2009; Oddo et al., 2009), which is now part of the MyOcean Project (www.myocean.eu, www.gnoo.bo.ingv.it/mfs/myocean/description.html). This dataset, available since 1999, consists of daily means of the northward and eastward current velocity components $U_{MFS} = (u_{MFS}, v_{MFS})$ on 72 unevenly vertical levels (ranging from 1.4 m to 5000 m depth), with a horizontal resolution of $1/16^\circ \times 1/16^\circ$ (ca. 7 km × 7 km). We stress that to simulate the reverse time flowing, the main velocity field considered in the simulations was $-U_{MFS}$, and from now on we shall refer to U_{MFS} as the reversed velocity field.

Two additional velocity fields are superimposed to recover the short time and small spatial scale variability in the larval transport. The

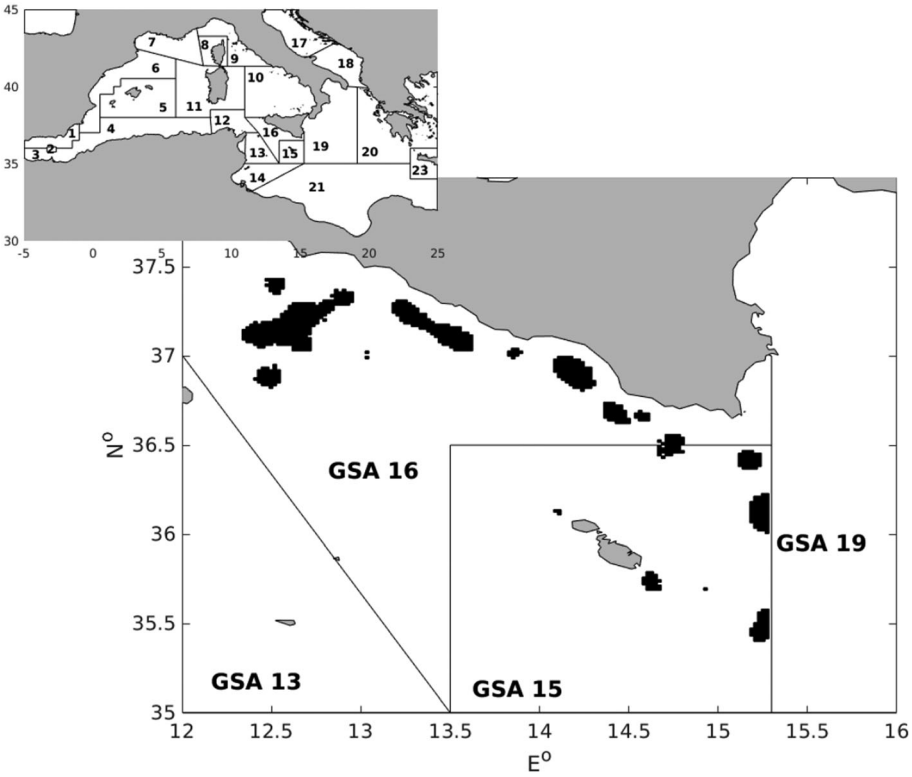

FIGURE 2 The nursery areas (colored in black) of deep-water rose shrimp in the Sicilian–Maltese shelf (GSA 15 and 16). The boundaries of GSAs are also shown

first field, the $U_{2D} = (u_{2D}, v_{2D})$ field *is* obtained from the stream function

$$\Psi = \frac{A}{k}[k(x\text{-}\varepsilon sin(\omega t))][k(y\text{-}\varepsilon sin(\omega t))]$$

that is, $\partial_x \Psi = v_{2D}$ and $\partial_y \Psi = -u_{2D}$, where $A = .1$ m/s, $\varepsilon = .1 l_0$, $\omega = 2\pi A_0 / l_0$ and $k = 2\pi / l_0$; $l_0 = 20$ km. The effect of the superposition of U_{2D} is to create some small scale disturbances, variable in time, typical of the chaoticity of the marine currents. The second superimposed velocity field is a 3D field used to restore the vertical mixing due to small (order 10 m) eddies characterizing the highly nonlinear dynamics of the Mediterranean basin (Pinardi & Masetti, 2000). This field, namely, $U_{3D} = (u_{3D}, v_{3D}, w_{3D})$, is obtained from the potential vector $\Phi = (\Phi_1, \Phi_2)$ as $\partial_z \Phi_1 = u_{3D}, \partial_z \Phi_2 = -v_{3D}, -\partial_x \Phi_1 + \partial_y \Phi_2 = w_{3D}$. The components (Φ_1, Φ_2) are defined according to

$$\Phi_1 = A_1 k_1 \sin[k_1(x - \varepsilon_1 \sin(\omega_1 t))]\sin[k_1(y - \varepsilon_1 \sin(\omega_1 t))],$$

$$\Phi_2 = A_2 k_2 \sin[k_2(x - \varepsilon_2 \sin(\omega_2 t))]\sin[k_2(y - \varepsilon_2 \sin(\omega_2 t))],$$

where $A_1 = .036$ m/s, $\varepsilon_1 = .2 l_1$, $\omega_1 = 2\pi A_1 / l_1$, $k_1 = 2\pi / l_1$, $A_2 = .041$ m/s, $\varepsilon_2 = .2 l_2$, $\omega_2 = 2\pi A_2 / l_2$, $k_2 = 2\pi / l_2$ where $l_1 = 30$ m and $l_2 = 42$ m.

Finally, the time evolution of the Lagrangian particles is obtained by the system of equations

$$\begin{cases} \dfrac{dx}{dt} = u_{MFS}(r,t) + u_{2D}(r_c,t) + u_{3D}(r_c,t) \\ \dfrac{dy}{dt} = v_{MFS}(r,t) + v_{2D}(r_c,t) + v_{3D}(r_c,t) \\ \dfrac{dz}{dt} = w_{3D}(r_c,t) \end{cases}$$

where $r(t) = (x(t), y(t), z(t))$ is the position vector (longitude, latitude and depth), and $r_c(t) = (x_c(t), y_c(t), z_c(t))$ are the relative coordinates computed in the reference frame of the mass center of two initially close particles in the so called *quasi*-Lagrangian approach, according to which each pair of initially closed particles moves in its own kinematic field anchored to its mass center advected by the main current velocity field U_{MFS}, and the small-scale dispersive effects are governed by the velocity field U_{2D} and U_{3D}.

The depth $z(t)$ of a specific particle is also subject to a forcing factor introduced to induce vertical migration dependent on larval-life cycle. The proposed approach follows that presented in Pires et al. (2021) for simulating the larval transport of the deep-water shrimp in the south-western Portuguese coast. In particular, during the first 15 days of simulations (last 15 days of the larval stage) particles were forced to move in the lower layers (below 100 m depth) and a bounce down effect was imposed when a particle hits the 100 m depth level from below. In the subsequent simulated stage, the particles were forced to move in an almost surface layer, above the 100 m of depth: in particular, only at the 16 day of simulation, a linear vertical velocity field is adopted in place of w_{3D} to favor the transport of each particles to the 100-m depth level. The w_{3D} is then restored with a bounce up effect when a particle hits the 100-m depth level from the above up to the last day of simulation (early 24 h of life): here, a linear vertical velocity field was imposed to force the particles to reach the bottom of the water column.

The above model was tested in the past and calibrated to capture most of the hydrodynamic features of the studied area. Actually there are only sensitivity/reliability analyses of the model for forward-in-time simulations. Concerning the predictivity of the model, Palatella et al. (2014) performed an analysis of the root mean square separation between the real trajectory of experimental drifters obtained from the ARGO program, showing the good predictive behavior of the model (see Appendix A of the work). Gargano et al. (2017) demonstrated that the same model was able to reproduce the distribution of the persistent areas of red mullet settler concentrations identified in the SoS (Garofalo et al., 2011). Analysis on the sensitivity of the model was also reported in Gargano et al. (2017), where the authors have shown that the model is only weakly sensitive to the variation of the main parameters, and that the main role in the dispersive process is played by the U_{3D} field with its induced vertical mixing and small-scale vortical structures. Furthermore, Lacorata et al. (2014) tested the model with only the U_{2D} field against the real drifter data. They showed that the U_{2D} field allows, in part, to recover the error induced by the unresolved scales not present in the velocity field U_MFS, and a further refinement of the resolved scales does not induce appreciable improvements in the predictability of the model.

2.4 | The initial setup

The time period selected for running simulations was 2005–2015, long enough to observe both seasonal and inter-annual variability of the currents circulation patterns in the entire SoS (Pinardi et al., 2015) and different AIS regimes linked to cyclonic and anticyclonic circulation of the Ionian sea.

As we are interested in determining the relevant spawning areas of DPS in the SoS, simulations were performed to capture two peaks of spawning, in spring/summer and autumn/winter (Bianchini et al., 2010), two periods which also take into account the seasonality of AIS and ATC. In addition, simulations were performed for two different periods of development of the DPS larval phase (Heldt, 1938; Pires et al., 2021), that is, 45 and 65 days, hereafter called scenario S_{45} and S_{65} respectively. The S_{45} was decided considering the average value of the only information available on the development period of the DPS larval phase (Heldt, 1938; Pires et al., 2021), while the S_{65} was chosen to simulate a more favorable situation for larval dispersion compared to S_{45}, and therefore to consider an increased connectivity between the Sicilian–Maltese shelf and contiguous areas.

In summary, we randomly placed 1200 pairs of drifting particles (i.e., recruits) in the known nursery areas of the SoS (Figure 2), each day for the two periods July 10–30 and February 8–28, and followed

their backward-in-time trajectories for 45 days to configure the S_{45}-Spring/Summer and S_{45}-Autumn/Winter scenarios respectively. For the S_{65}, the same amount of particles per day was released in the two periods July 25 to August 15 and February 23 and March 8 to 9 (depending on the bissextile years), each of them followed backward-in-time for 65 days to configure the S_{65}-Spring/Summer and S_{65}-Autumn/Winter scenarios respectively. The particles were randomly released in the known nursery areas at the bottom of the water column and they were driven by the velocity field introduced in the previous section. The numerical solutions of the Lagrangian system were obtained by using a fourth order Runge–Kutta temporal scheme (Lambert & Lambert, 1991) with a time step of $dt = 120$ s.

As the velocity field U_{MFS} is given on the model's spatial grid each day, the exact value $U_{MFS}(r(t))$ in $r(t)$ was obtained through a horizontal bilinear interpolation, using the nine grid cells surrounding the position $(x(t), y(t))$, and a vertical linear interpolation between the two depth levels bounding $z(t)$ at each time step. As U_{MFS} has temporal discontinuity at 00:00 AM, when passing from 1 day to another, U_{MFS} was linearly weighted between two consecutive days from 08:00 a.m. to 00:00 a.m. (following the backward-in-time evolution) so that the velocity field of a specific day smoothly changed to that of the following day. Finally, if a particle was driven toward the coast, it rebounded to its previous position, by means of a reflective boundary condition imposed along the basin boundaries.

2.5 | Larval transport success

The Geographical Sub Areas (GSAs) defined by the GFCM in the Mediterranean Sea for fisheries management purposes (FAO-GFCM, 2009) were adopted as spatial units to which the recruits origin is attributed (Figure 2).

To determine the most relevant GSAs (sources) that feed the DPS nurseries of the northern SoS, we defined an index related to each GSA in the period analyzed, hereafter named *GSA transport coefficient* (GTC).

The GTC was computed following the procedure initially developed by Huret et al., 2007 and applied in the SoS for determining the larval transport success of the early stages of red mullet (Gargano et al., 2017). In particular, naming $GTC^k_{i,j}$ the GTC over the specific kth GSA (k ranging from 1 to 30) for the generic particle i initially released in the year j, the $GTC^k_{i,j}$ is defined as the portion of time (values in the range [0,1]) that a particle spends over the selected GSA in its first D days of life, that is, the last D days of the simulated backward-in-time trajectory of the particle: we set $D = 10$ for the S_{45} scenario, and $D = 15$ for the S_{65} scenario. This portion was evaluated as the ratio between the sum of the days a particle spends over a GSA during the last D days of the simulated trajectories and D (actually we check for the position of a particle every 6 h to obtain a more refined result with 60 samples). The global GTC for a specific GSA in the period 2005–2015 is then computed as the mean value of the various $GTC^k_{i,j}$ over the years and the number of particles. In particular, the GTC for the kth GSA is given by

$$GTC^k = \left(\sum_{j=2005}^{2015} \frac{\sum_i GTS^k_{i,j}}{N_j} \right) / 11,$$

where N_j is the total number of particles released in the year j, and the internal summation over the index i can be considered as an annual GTC for the kth GSA. This index measures the contribution of each GSA to the recruitment.

To measure the inter-annual variability of the results we also computed the coefficient of variation (CV) of the GTC defined as the ratio between the standard deviation and the mean of the various GTC^k.

2.6 | Hotspot analysis of the spawners

A hotspot analysis was performed to identify the spatial patches defining potential spawning areas. The region $\Omega = [5°\text{E}, 20°\text{E}] \times [31°\text{N}, 42°\text{N}]$ was chosen for the investigation, as it contained all the simulated trajectories. Region Ω was divided in $1/8° \times 1/8°$ (14 km × 14 km) cells excluding the inland cells. For each year, we first counted, every 6 hours, the total number of particles within each cell during their last 10 or 15 days of backward transport depending on the scenario (first 10 or 15 days of life). Each count was multiplied by a weight $w(z)$ (value in [0,1]) related to the depth z of the specific cell, in order to filter the results according to the probability that the spawners (the source of recruits) occur at a specific depth. This weight was computed from the distribution of the density index in Spring of the mature females (number of specimens/km^2) as a function of the depth presented by Fortibuoni et al., 2010, and assuming that the standardized index is a two-piecewise Gaussian function given by

$$w(z) = \begin{cases} \exp\left(-(z-\mu)^2/{\sigma_1}^2\right), & z < \mu \\ \exp\left(-(z-\mu)^2/{\sigma_2}^2\right), & z \geq \mu \end{cases}$$

Nonlinear least square fitting procedures returned the values $\mu = 183$, $\sigma_1 = 51, \sigma_2 = 83$.

The total weighted counting allowed to retrieve in each cell and for each year an abundance index. Hence, the Getis-Ord gi* analysis (Getis & Ord, 1992) was applied to identify the spawners hotspots in the region Ω through the analysis of the z score (or p level) values, where z score value in each cell was determined by averaging the eight neighboring cells. To mark a cell as hotspot for a specific year we selected cells having a z-score greater than a given threshold value, fixed after various trials to $z_{thr} = 3$. This value was considered the optimal trade-off for filtering out cells where most of the particles were highly concentrated without marking an unrealistic number of cells as hotspot. Once we marked the hotspot cells in each year, we computed the ratio of the number of years in which a cell is a hotspot to the total number of years, obtaining a value between 0 and 1 for each cell that can be interpreted as a persistence index (PI).

Finally, to prove the validity of the backward-in-time approach, we performed several forward-in-time simulations (see Supplementary material) aimed to follow trajectories of particles released in the final positions of the backward-in-time simulations and verify the return fidelity of the particles to the starting position (nursery areas of the northern SoS; Figure S3).

3 | RESULTS

The numerical simulations performed for the two scenarios of larval duration S_{45} and S_{65} in the two seasons allowed to recover GTC values greater than zero for 10 GSAs of the central Mediterranean (Figure 3 and Tables S1 and S2). The main differences arise between the two seasons, and although the S_{45} and S_{65} scenarios show qualitatively similar values of GTC, some peculiar differences can be observed.

The results mainly indicate that, regardless the season and the scenarios, the main GSA feeding the nurseries of the northern SoS (Figure 2) is GSA16, which shows the highest GTC values in each year. In particular, GTC varies between .32 and .8, being, on average, lower in the winter period (Tables S1 and S2). In Figure 3 the mean GTC is shown for the various configurations: it can be observed that during the Spring/Summer it is just above .6 for both scenarios, whereas in the Autumn/Winter the mean values of GTC decrease to .43 and .56 for the S_{65} and the S_{45} scenarios respectively.

The secondary sources of recruits settled in the northern SoS are GSAs 12, 13, 15, but it is interesting to note that their contribution differs according to the season. In fact, GSA 15 is on average the main secondary source during the Spring/Summer (GTC .12 and .14 for the S_{65} and S_{45} respectively), followed by GSAs 13 (GTC .07 and .06) and GSA 12 (GTC .08 and .05) (Figure 3). On the contrary, the average GTC of GSA 15 decreases during Autumn/Winter (GTC .10 and .11), while the other GSAs acquire importance as secondary suppliers of recruits to the Sicilian–Maltese shelf, in the order GSA 13 (GTC .16 and .15) and 12 (GTC .11 and .07). Finally, the residual contribution is given by GSAs 4, 10, 11, 14, 19, and 21 with average GTC values less than .05 in both scenarios and both seasons.

Interesting information on the inter-annual variability of the GTC is provided by the CV (Figure 4). In most configurations, the CV is highest in the S_{45} scenario and mainly in the Spring/Summer season. The GSA 16 differs clearly from all the others GSAs for having the lowest CV, below .25 in all the configurations. The GSA 15 exhibits

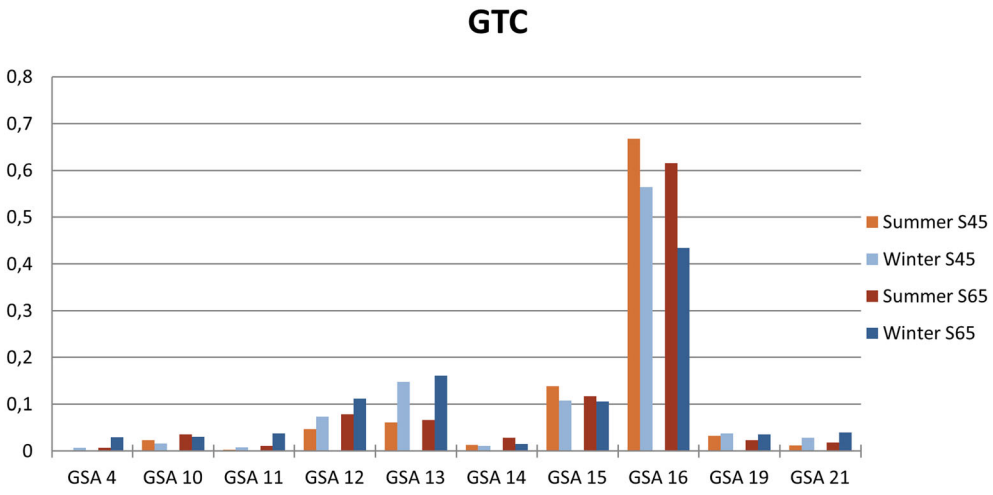

FIGURE 3 Average GSA transport coefficients (GTC) in 2005–2015 computed for various GSAs and different scenarios

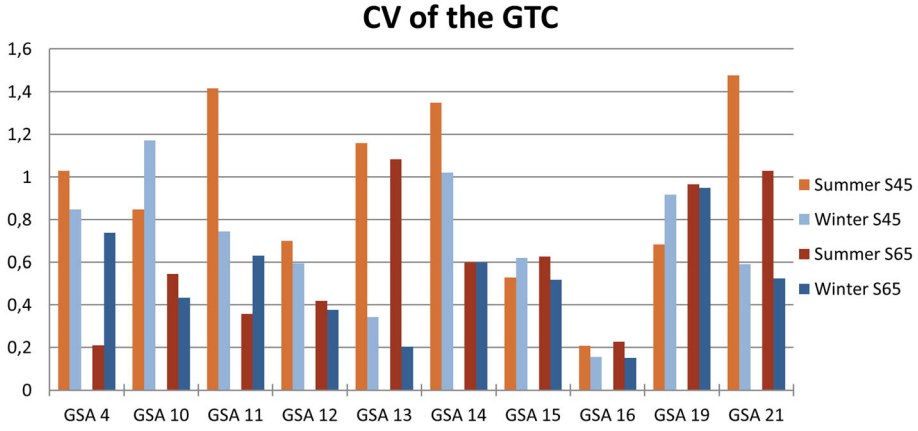

FIGURE 4 The coefficient of variation (CV) of the GSA transport coefficient (GTC) reported in Figure 3

similar CVs across configurations, ranging from .5 to .6. The GSA 12 shows CVs of approximately .4 in the S_{65} scenario and in the range .6–.7 for the S_{45} scenario. Finally, a particular result is observed for GSA 13 that has CVs greater than 1 in Spring/Summer and less than .4 in the winter season. With a few exceptions, all the other GSAs, showing GTC less than .05, have CVs greater than .6.

The PI maps of the spawners aggregation in the region of interest are shown in Figure 5 for all the configurations. Some common patterns can be observed. The hotspot regions in the S_{65} scenario are broader than in the S_{45} scenario. In all cases, regardless the season, a large hotspot in the GSA 16, labeled *H1* in the maps, is identified in the south-western corner of Sicily and expands from the coast between Mazara del Vallo and Licata toward the open sea reaching the Maltese coasts. Another hotspot in the GSA 16, common to all scenarios and seasons, is *H2* that is connected with *H1* but centered close the Egadi Islands. Finally, another small hotspot in the GSA 16, *H3*, is located in the south-eastern corner of Sicily, near Syracuse, with slightly detached hotspots, *H3*b, clearly observable only during the Autumn/Winter.

The main difference between the two seasons lies in the hotspots found far from the southern coast of Sicily and close to African coasts. During the Autumn/Winter, a wide region straddling the GSA 16 and 13, *H4*, with the centroid off the Gulf of Hammamet, extends north-west up to the Galite bank, and south-east beyond Lampedusa. This hotspot has a significant PI during Autumn/Winter, whereas during Spring/Summer it appears fragmented with only small parts having significant PI. Finally, the hotspot *H5* in the *GSA 15* is well identified off Tripoli and parallel to the African coast for the S_{65}, while in the S_{45} scenario it is only barely visible.

The last 15 days of some simulated backward-in-time trajectories (corresponding to the first 15 days of life of the larvae), selected from those found in a habitat suitable for spawning (depth less than 200 m), are shown in Figure 6 for both seasons of the S_{65} scenario. Only trajectories from the main feeding GSAs (12-13-15-16) are shown. Particles arriving from GSA 12 usually start near the border between Algeria and Tunisia, while those from GSA13 are initially distributed in the large area between Hammamet and Lampedusa. Particles from GSA 15 are initially located off the south-eastern corner of

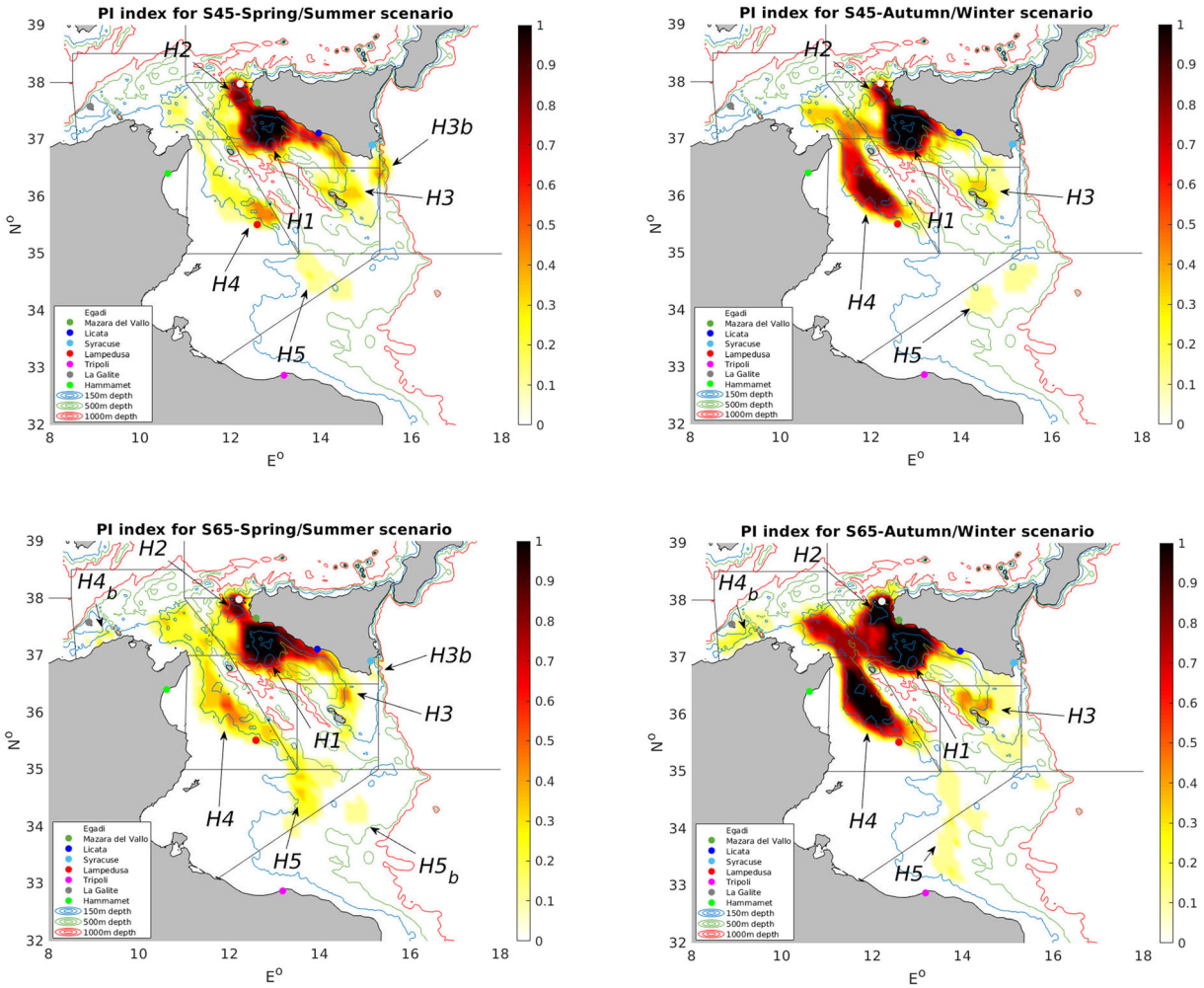

FIGURE 5 Persistent hotspots (labeled from H1 to H5) of spawners supplying larvae of DPS to GSA 15 and 16 in the different scenarios. The persistence index (PI) is computed over the period 2005–2015

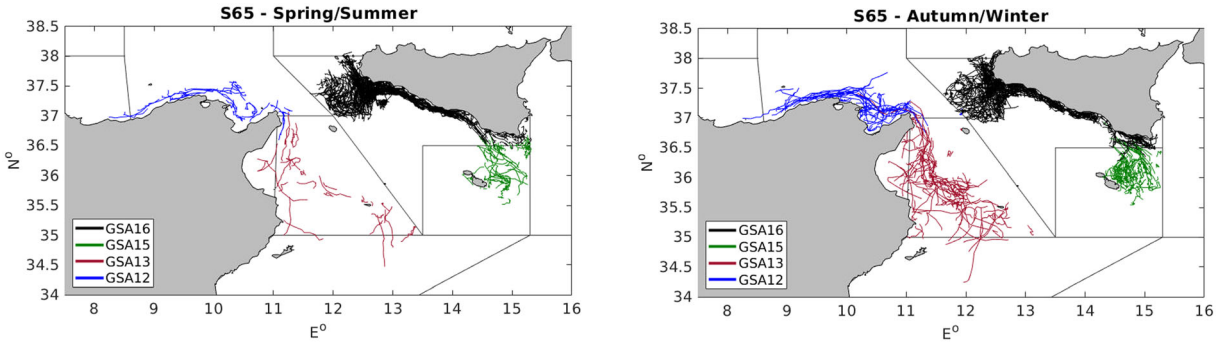

FIGURE 6 Trajectories of the particles in the first 15 days of life (i.e., the last 15 days of numerical simulations) for the S_{65} scenario, selected from those found in a habitat suitable for spawning (depth <200 m). Only the trajectories from GSAs with the highest GTC (GSA transport coefficient) are shown and are colored according to the potential GSA of origin

Sicily. In the GSA 16, the particles initially travel along the southern coast of Sicily and off the south-western corner (where the semi-permanent cyclonic vortex is present): these trajectories closely describe the vertical dynamics induced by the vortex. A similar pattern was obtained for the S_{45} scenarios, not shown here.

To extend and complete the representation of the typical dynamic pattern of particles, some complete trajectories for the various scenarios are provided as supporting information (Figures S1 and S2).

4 | DISCUSSION

The Strait of Sicily is a relevant area of the Mediterranean Sea for demersal fisheries that need effective management measures. Here we focused on the deep water rose shrimp that is managed as a straddling stock, due to poor information on its spatial structure. Gaining information on the stocks structure and on the connectivity between population units is thus essential to solve the mismatch between biological and management units and identify the appropriate geographical scales for stock assessment and management (e.g., Cadrin, 2020; Fiorentino et al., 2014; Hidalgo et al., 2019; Melaku Canu et al., 2020).

Historically, most studies on larval dispersal and connectivity in the Mediterranean have focused on small pelagic fish resources (e.g., Nicolle et al., 2009; Palatella et al., 2014), as their annual recruitment success strongly relies on oceanographic conditions, and on coastal fish (e.g., Calò et al., 2018; Legrand et al., 2019; Torrado et al., 2021), as this information is critical for the effective design of Marine Protected Area networks (Di Franco et al., 2012). However, in recent years, studies on the connectivity between spawning and nursery areas of deep-sea demersal species have been receiving increasing attention for two main reasons, on the one hand to shed light on recruitment dynamics and improve the reliability of stock assessments (Hidalgo et al., 2019), on the other hand to assist in the implementation of spatial fisheries management measures for the protection of critical habitats in the open sea (Russo et al., 2019).

Our study presents for the first time the application of a backward-in-time Lagrangian dispersal model aimed to investigate where the recruits of DPS, settled in the northern side of the SoS (GSAs 15 and 16), come from, that is, where the spawners that provide successful recruitment are located. Answering this question is crucial in assessing whether the DPS population of the northern SoS can be managed as a single stock. The main results of simulated trajectories suggest that contribution of larvae produced within the GSA 16 is predominant over contribution from surrounding areas. A minor contribution is due to potential spawning areas located in GSA 12, 13, and 15, and it is stronger in winter for the first two GSAs and in summer for GSA 15 in both scenarios of larval duration (Figure 3).

The very low inter-annual variability (CV) observed for GTC in GSA 16 supports the stable role over the years of the spawning grounds of this GSA in feeding the nurseries of the northern SoS. At the same time, GSAs 15, 12, and 13, which appear to be secondary sources of larvae, show high inter-annual variability, especially in the Spring/Summer season, consistent with the typical variability of AIS in the SoS. In fact, it is widely recognized that AIS is linked to the circulation reversal between cyclonic and anticyclonic regime in the Ionian Sea, a phenomenon that has been observed a few times in the period examined (Gačić et al., 2014).

Overall, our results are consistent with previous findings on DPS from Quattrocchi et al. (2019) who described the connectivity within the SoS as modulated by the decadal variability of the south-central Mediterranean Sea circulation, with a strong retention component of particles in the GSA 16 favored during the period of cyclonic circulation in the northern Ionian Sea and weaker AIS. Notably, recruitment in the east sector (Malta Bank, GSA 15) resulted always dependent on spawning in the west sector (Adventure Bank, GSA 16) in addition to the local spawning component.

The hotspot analysis allowed to identify the most persistent potential spawning areas and to highlight the hydrological features driving the observed spatial pattern, given the initial conditions, that is, the location of the nurseries along the Sicilian–Maltese shelf (GSA 15 and 16). In fact, the semi-permanent vortex (clockwise according to the backward-in-time simulation) lying over the Adventure Bank, is

the main responsible for the clockwise recirculating pathways of the particles in this area, leading to the detection of the spawning hotspot *H1* (Figure 5). This feature is however less evident during Autumn/Winter season, when the vortex over the Adventure bank is unstable and the marine current field is more variable, providing a possible explanation of the more fragmented hotspots we have retrieved during this season, as compared to the Spring/Summer.

Most of the particle pathways start from the nurseries located along the Sicilian coasts, showing a high local retention of eggs/larvae, while a minor part starts from the Maltese nurseries (Figures S1 and S2). Moreover, as a consequence of the eastward meandering of AIS along the Sicilian–Maltese shelf, backtracking of larvae leads to the detection of hotspots *H2* and *H3* (Figure 5); pathways ending in these hotspots were mainly originated from nurseries located in the eastern edge of the Malta Bank (Figures S1 and S2). The potential spawning areas located within GSA 16 (H1 and H2) were identified as the main source of young DPS recruited in the Sicilian–Maltese shelf with very low inter-annual and seasonal variability (Figure 4). Further pathways of larvae drifting from the south-east side of the Sicilian–Maltese shelf to the south-west side, after interacting with recirculation of currents in the Adventure Bank leads to the identification of the spawning hotspots *H4* and *H5* along the African shelf, which partially contribute to the network of nurseries in the northern SoS. The contribution of the hot spot along the Tunisian shelf is stronger in winter when the AIS is weaker and the ATC stronger (Béranger et al., 2004; Sorgente et al., 2003).

It is worth noting that these findings appear to be well supported by previous knowledge, suggesting a good predictive ability of our model. Indeed, the hotspot of spawners in the Sicilian–Maltese shelf (H1, H2, and H3 in Figure 5) fits well with spawning areas identified in previous works (Colloca et al., 2013; Fortibuoni et al., 2010). On the other hands the hotspot found along the Tunisian coast are consistent with the position of spawning areas preliminary identified using Local Ecological Knowledge of Captains of the distant trawlers of Mazara del Vallo fleet operating in the SoS (Fiorentino et al., 2019).

An attempt to schematize the connectivity pattern between the known nurseries in the northern SoS and the predicted location of the spawning areas backward-simulated by the Lagrangian model is given in Figure 7. It appears that the westernmost spawning areas within GSA 16 are highly connected by the AIS to nurseries located downstream along the Sicilian–Maltese shelf (GSA 16 and 15), in agreement to what found by Quattrocchi et al. (2019). In addition, a weak connectivity is observed between the northern and southern sectors of the SoS as nurseries of GSA 15 and 16 may be supplied secondarily and mainly in winter by spawning grounds located on the African shelf in GSA 12 and 13.

Some evidence of connectivity between the northern and southern sectors of the SoS had already been provided by Quattrocchi et al. (2019) using a forward Lagrangian dispersion model. Indeed, assuming a pelagic larval duration ranging between 10 and 60 days, the Authors predicted a weak exchange of larvae originating in spawning regions of the northern SoS with the nurseries off the Tunisian coast. This was explained by the seasonal and inter-annual circulation variability that makes the AIS jet, which is a potential barrier to the exchanges of flow and larvae between the Northern and Southern SoS, only partially stable.

Further evidence of the exchange rate between the European and African sides of the SoS has been recently provided by Falcini et al. (2020) who used backward-in-time simulations to assess the putative location of spawning grounds of European anchovy within the SoS and adjacent areas over the period 2009–2012. Their findings are consistent with our results and highlight a certain level of connectivity between the northern SoS and GSA 12 although characterized by high temporal variability, as well as a minor and equally variable potential contribution due to GSAs 11, 19. The authors performed the analysis both by applying a filter based on the concentration of chlorophyll-a to find suitable habitats for the spawners, and without filtering the simulated trajectories. In conclusion they suggested that the connectivity between the GSA 12 and the northern SoS is supported by the meandering structure of the AIS that bridges the

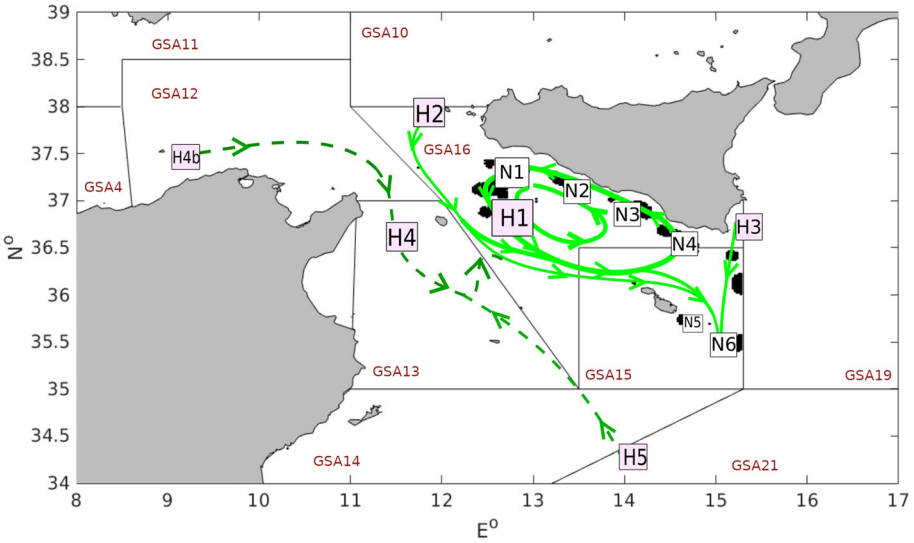

FIGURE 7 Schematized representation of the connectivity pattern (green lines) between the hotspots (H) and the nurseries (N) of DPS as retrieved from the numerical simulations. The direction of the arrows follows the standard forward-in-time dynamics. Solid lines indicate persistent pathways in both scenarios, dashed lines indicate pathways detected only in S_{65} scenario

Tunisian and Sicilian shelves, and reinforced by chlorophyll-rich pathways.

The importance of filtering the results of the backward-in-time Lagrangian models considering ecological factors which can affect the biological cycle of the species, was recently discussed by Legrand et al. (2019). According to the authors, the use of information such as environmental factors triggering spawning (e.g., chlorophyll-a introduced by Falcini et al., 2020) or any constraint restricting spawning behavior of the species (e.g., depth limit used in our study) together with other biological traits of the species is critical in order to find the effective sources of larvae among all potential sources. Therefore, the more detailed information is available about the biological traits of the species, the more refined is the quantitative characterization of dispersal and connectivity patterns.

We cannot exclude that some methodological choices that were adopted in our study could potentially have influenced the observed larvae dispersal pattern. First, the vertical ontogenetic migration of the larvae and, second, the reflective condition at the coastal boundary. As discussed below, to shed more light on the effects of these assumptions, we ran a few simulations considering the opposite conditions, that is, no vertical movement of larvae and their full beaching/stranding on the coast.

In the present study, the vertical ontogenetic migration of larvae was simulated based on the life cycle phases and vertical movement of the larval stages described in Pires et al. (2021). According to this scheme, we forced the particles to move below 100 m depth during the last 15 days of the larval stage (first 15 days of simulation). This can strongly influence the dispersion process, as the intensity of sea currents varies according to depth and season. Since the AIS, the main sea current governing the large-scale velocity field of our model, is most intense in the depth range 13–30 m and weakens with depth (Sorgente et al., 2011), forcing the vertical movement of the particles in the lower layers could promote retention and reduce dispersion (Calò et al., 2018). This is just what we have observed by comparing the results presented here with preliminary numerical simulations performed without introducing vertical movement for the S_{65}-Spring/Summer scenario in the period 2005–2009: the dispersion was stronger, with, on average, a smaller GTC for the GSA 16, and a larger GTC for the GSA 19 and especially the GSA 11 which resulted a secondary relevant GSA similarly to the GSAs 12–13. This confirms the need to improve knowledge on larval biology and in particular on active vertical displacement. We also want to stress the importance of introducing a proper vertical movement, otherwise, as already shown in Palatella et al. (2014), the individual vertical motility could be less than or comparable to turbulent mixing intensity (ruled by the 3D velocity field in our model), and thereby not influencing the overall results.

The interactions of Lagrangian particles with the coastal boundary, could affect the dynamics of dispersal. In our simulations, similarly to what is generally done in larval dispersal studies (e.g., Melaku Canu et al., 2020; Palatella et al., 2014), we did not consider larval beaching/stranding on the coast but we applied reflective boundary conditions that, depending on the geometry of the domain, the run length and the strength of the velocity field, could affect the GTCs and the hotspot regions. Many models based on Lagrangian computations, analyzed the stranding effect, showing that the stranding probability of particles may be meaningful, especially in conjunction with the particle resuspension probability (see Hinata et al., 2020; Liubartseva et al., 2018; Onink et al., 2021 for applications to marine plastic debris), and the vertical migration (see Berline et al., 2013). However, the stranding effect (mainly applied to the dispersal of pollutants in the cited papers) has a strong impact on Lagrangian simulations in the long run, and becomes quite relevant after months (Mansui et al., 2015; Onink et al., 2021). Due to the relatively low-medium length of our simulations, it should be expected that boundary conditions do not affect the results we have obtained. Indeed, numerical simulations performed on the year 2015 with a full beaching conditions, have revealed only a slight decrease in the GTC of GSA 16, with a maximum effect in the S_{65}-Spring/Summer scenario (GTC of .71 against .79 obtained with the reflective boundary condition). Palatella et al. (2014) achieved a decrease in their Lagrangian transport index of the same order of magnitude as ours when they tested the sensitivity of their model (the same one we used) to a change from coastal reflection to beaching (their experiment called RUN T4).

The aspects related to biological connectivity in the marine environment are complex and dispersal processes are certainly among the main factors promoting the exchange of individuals between populations (Cowen & Sponaugle, 2009). Knowledge of the population structure is important in order to take effective management measures in response to fishing, environmental pressures and climate change. A population structure composed of several subunits interconnected through larval dispersal and adult migrations is consistent with the so-called metapopulation model (Fogarty & Botsford, 2006). According to Cadrin et al. (2014) a metapopulation is a system of interacting biological populations, termed subpopulations, which exhibit a degree of independence in local population dynamics as well as connectivity between subpopulations. Overall, the dynamic of metapopulations depends on trends of individual subunits and on the connectivity between them. Kerr et al. (2017) has shown that spatial structure and connectivity (both in terms of larval dispersal and fish migrations) within and between populations' units affected strongly the productivity (spawning-stock biomass, SSB), stability (variation in SSB), resilience (time to rebuild SSB after environmental disturbance), and sustainability (maximum sustainable fishing mortality and yield) of exploited populations. The exploitation by fisheries of a metapopulation could cause the over-exploitation of the less productive subunits and/or the under-exploitation of more productive ones, impeding stability and resilience of the whole metapopulation to human and environmental pressures (Kerr et al., 2017).

Due to the poor knowledge of its population structure in the SoS DPS is currently managed as a single straddling stock inhabiting both the European and African shelf and the deep waters in the middle of the SoS, thus covering all GSAs 12–16 (Fiorentino et al., 2013). Our results support the presence of a population having a more complex structure composed of several subunits connected by dispersion

pathways. Nurseries in the northern SoS (GSAs 15 and 16) are mostly furnished by potential spawning areas located within GSA 16 at distances varying from tens to hundreds of kilometers. However, a wider dispersal pattern seems to act as well, with larvae coming from potential spawning areas located in more distant areas, precisely the GSAs 12, 13, and 15 whose role in the recruitment dynamics is modulated by the inter-annual and seasonal variability of circulation and the pelagic larval duration. This large scale but weak connectivity is coherent with the absence of sharp genetic differences in the DPS populations of the Mediterranean Sea found by Lo Brutto et al. (2013). The authors observed a pattern of gradual genetic differentiation along a west–east axis in the Mediterranean basin arising as geographic distance increases (Isolation by Distance model). The role of both hydrodynamic and biological factors is crucial in explaining this pattern. Over long distances, on the one hand the hydrodynamic factors do not act sufficiently to prevent differentiation while on the other hand the features of the dispersion processes (pelagic phase duration and mortality of larvae) do not guarantee homogenization (Lo Brutto et al., 2013).

The dynamic behavior of the different subunits forming the metapopulation of DPS in the SoS is expected to depend on the reactions of individual local sub-populations to environmental factors and exploitation, as well as on the connectivity between these population subunits. By examining the effects of the mismatch between the true spatial structure of exploited populations and the management units, Cadrin (2020) has shown that conventional stock assessments of spatially structured populations have failed to detect overfishing and depletion of less productive population subunits. Instead, considering the population spatial structure in stock assessments promotes the conservation of all components of the population and the management of sustainable and productive fisheries.

Our study has gone some way toward enhancing our understanding of the population structure of DPS in the SoS but the picture is still incomplete and research is needed to cover knowledge gaps in the southern SoS. Indeed, detailed information on the nursery and spawning areas off the African coast is still missing, as well as genetic analysis extended to populations of the North-African shelf. Another important limitation is the scarce knowledge on DPS larval duration, which is a critical parameter to setting up Lagrangian dispersal models. Some authors have supported the use of a combination of complementary approaches to increase the accuracy of larval dispersal analyses, in particular they have used otolith microchemistry as natural tags to study the dispersal history of fish (Di Franco et al., 2012) and validate the connectivity patterns resulting from the Lagrangian dispersal models (Calò et al., 2018; Legrand et al., 2019) or the daily growth rings to estimate the pelagic larval duration (Torrado et al., 2021). Unfortunately, these techniques cannot be used in crustacean species lacking of hard structures such as otoliths. Finally, further work is needed to gather more information on biological traits of species, including spawning strategy and preferential habitat (Legrand et al., 2019) and larvae biology (growth, mortality and vertical migration), in order to make connectivity models more realistic (Melaku Canu et al., 2020; Ospina-Alvarez et al., 2012). These are all important issues for future research and will improve our understanding of the spatial structure and connectivity between subpopulations of this valuable commercial species throughout the SoS and surrounding areas.

Spatial measures for fisheries management, in terms of protection of the main nursery areas of DPS, have been adopted by GFCM in the northern sector of the SoS (Russo et al., 2019), and thus, understanding how the different spawning areas contribute to the replenishment of these nurseries is becoming more and more relevant. Our results have shown that spawning grounds occurring in the GSA 16 contribute more than those of the other GSAs of the SoS (GSA 12, 13, and 15) to the high productivity and resilience of DPS fishery off the southern coast of Sicily and therefore they need a special protection. In our view, this also implies that the current approach that assumes DPS as a single stock for assessment and fishery management in the SoS, without considering its spatial structure, should be revised.

ACKNOWLEDGMENTS

This work has been supported by the European Commission-Directorate General MARE (Maritime Affairs and Fisheries) through the Research Project MANTIS: Marine protected Areas Network Towards Sustainable fisheries in the Central Mediterranean [MARE/2014/41—Ref. Ares (2015)5672134-08/12/2015]. Open Access Funding provided by Consiglio Nazionale delle Ricerche within the CRUI-CARE Agreement.

CONFLICT OF INTEREST

The authors state that there are no conflicts of interest to declare.

AUTHOR CONTRIBUTIONS

F.F., F.G., and G.G. conceived the ideas and designed the study. F.G. developed the model and analyzed the data. All the authors discussed the results and wrote the paper. All authors gave final approval for publication.

DATA AVAILABILITY STATEMENT

The data that support the findings of this study are available from the corresponding author upon reasonable request.

ORCID

Francesco Gargano https://orcid.org/0000-0002-6453-4883
Germana Garofalo https://orcid.org/0000-0001-9117-6252
Federico Quattrocchi https://orcid.org/0000-0002-2030-5640
Fabio Fiorentino https://orcid.org/0000-0002-6302-649X

REFERENCES

Abellò, P., Abella, A., Adamidou, A., Jukic-Peladic, S., Maiorano, P., & Spedicato, M. T. (2002). Geographical patterns in abundance and population structure of *Nephrops norvegicus* and *Parapenaeus longirostris* (Crustacea: Decapoda) along the European Mediterranean coasts. *Scientia Marina*, *66*(2), 125–141. https://doi.org/10.3989/scimar.2002.66s2125

Béranger, K., Astraldi, M., Crépon, M., Mortier, L., Gasparini, G. P., & Gervaso, L. (2004). The dynamics of the Sicily Strait: A comprehensive study from observations and models. *Deep Sea Research Part II: Topical Studies in Oceanography*, *51*(4–5), 411–440. https://doi.org/10.1016/j.dsr2.2003.08.004

Berline, L., Zakardjian, B., Molcard, A., Ourmières, Y., & Guihou, K. (2013). Modeling jellyfish *Pelagia noctiluca* transport and stranding in the Ligurian Sea. *Marine Pollution Bullettin*, *70*(1–2), 90–99. https://doi.org/10.1016/j.marpolbul.2013.02.016

Bianchini, M. L., Di Stefano, L., & Ragonese, S. (2010). Reproductive features of the deep-water rose shrimp, *Parapenaeus longirostris* (Crustacea: Penaeidae), in the strait of Sicily. *Mediterranean Marine Science*, *11*(1), 81–92. https://doi.org/10.12681/mms.92

Cadrin, S. X. (2020). Defining spatial structure for fishery stock assessment. *Fisheries Research*, *221*, 105397. https://doi.org/10.1016/j.fishres.2019.105397

Cadrin, S. X., Goethel, D. R., Morse, M. R., Fay, G., & Kerr, L. A. (2019). "So, where do you come from?" the impact of assumed spatial population structure on estimates of recruitment. *Fisheries Research*, *217*, 156–168. https://doi.org/10.1016/j.fishres.2018.11.030

Cadrin, S. X., Kerr, L. A., & Mariani, S. (2014). Interdisciplinary evaluation of spatial population structure for definition of fishery management units. In *Stock identification methods* (pp. 535–552). Academic Press. https://doi.org/10.1016/B978-0-12-397003-9.00022-9

Calò, A., Lett, C., Mourre, B., Pérez-Ruzafa, Á., & García-Charton, J. A. (2018). Use of Lagrangian simulations to hindcast the geographical position of propagule release zones in a Mediterranean coastal fish. *Marine Environmental Research*, *134*, 16–27. https://doi.org/10.1016/j.marenvres.2017.12.011

Ciannelli, L., Fisher, J. A. D., Skern-Mauritzen, M., Hunsicker, M. E., Hidalgo, M., Frank, K. T., & Bailey, K. M. (2013). Theory, consequences and evidence of eroding population spatial structure in harvested marine fishes: A review. *Marine Ecology Progress Series*, *480*, 227–243. https://doi.org/10.3354/meps10067

Colloca, F., Garofalo, G., Bitetto, I., Facchini, M. T., Grati, F., Martiradonna, A., Mastrantonio, G., Nikolioudakis, N., Ordinas, F., Scarcella, G., & Tserpes, G. (2015). The seascape of demersal fish nursery areas in the North Mediterranean Sea, a first step towards the implementation of spatial planning for trawl fisheries. *PLoS ONE*, *10*(3), e0119590. https://doi.org/10.1371/journal.pone.0119590

Colloca, F., Spedicato, M.T., Massutí, E., Garofalo, G., Tserpes, G., Sartor, P., Mannini, A., Ligas, A., Mastrantonio, G., Reale, B., & Musumeci, C. (2013). Mapping of nursery and spawning grounds of demersal fish. Mediterranean sensitive habitats (MEDISEH) Final Report, (2013) DG MARE Specific Contract SI2.600741, Heraklion (Greece).

Cowen, R. K., & Sponaugle, S. (2009). Larval dispersal and marine population connectivity. *Annual Review of Marine Science*, *1*, 443–466. https://doi.org/10.1146/annurev.marine.010908.163757

Crisiani, F., & Mosetti, R. (2016). Is the bimodal oscillating Adriatic-Ionian circulation a stochastic resonance? *Bollettino di Geofisica Teorica ed Applicata*, *57*(3), 275–285.

Cury, P. M., Fromentin, J.-M., Figuet, S., & Bonhommeau, S. (2014). Resolving Hjorts dilemma: How is recruitment related to spawning stock biomass in marine fish? *Oceanography*, *27*(4), 42–47. https://doi.org/10.5670/oceanog.2014.85

De Ranieri, S., Mori, M., & Sbrana, M. (1998). Preliminary study on the reproductive biology of *Parapenaeus longirostris* (Lucas) off the northern Tyrrhenian Sea. *Biologia Marina Mediterranea*, *5*(1), 710–712.

Di Franco, A., Gillanders, B. M., De Benedetto, G., Pennetta, A., De Leo, G. A., & Guidetti, P. (2012). Dispersal patterns of coastal fish: implications for designing networks of marine protected areas. *PLoS ONE*, *7*, e31681. https://doi.org/10.1371/journal.pone.0031681

Dos Santos, A. (1998). On the occurrence of larvae of *Parapenaeus longirostris* off the Portuguese coast. *Journal of Natural History*, *32*, 1519–1523. https://doi.org/10.1080/00222939800771051

Dos Santos, A., Santos, A. M. P., Conway, D. V. P., Bartilotti, C., Lourenço, P., & Queiroga, H. (2008). Diel vertical migration of decapod larvae in the Portuguese coastal upwelling ecosystem: Implications for offshore transport. *Marine Ecology Progress Series*, *359*, 171–183. https://doi.org/10.3354/meps07341

Falcini, F., Corrado, R., Torri, M., Mangano, M. C., Zarrad, R., Di Cintio, A., Palatella, L., Jarboui, O., Missaoui, H., Cuttitta, A., Patti, B., Santoleri, R., Sarà, G., & Lacorata, G. (2020). Seascape connectivity of European anchovy in the Central Mediterranean Sea revealed by weighted Lagrangian backtracking and bio-energetic modelling. *Scientific Reports*, *10*, 18630. https://doi.org/10.1038/s41598-020-75680-8

Falcini, F., Palatella, L., Cuttitta, A., Buongiorno Nardelli, B., Lacorata, G., Lanotte, A. S., Patti, B., & Santoleri, R. (2015). The role of hydrodynamic processes on anchovy eggs and larvae distribution in the Sicily Channel (Mediterranean Sea): A case study for the 2004 data set. *PLoS ONE*, *10*(4), e0123213. https://doi.org/10.1371/journal.pone.0123213

FAO-GFCM. (2009). GFCM resolution RES-GFCM/33/2009/2, establishment of geographical sub-areas in the GFCM area amending the resolution GFCM/31/2007/2. In: FAO General Fisheries Commission for the Mediterranean, Report of the Thirty-Third Session. Tunis, 23–27 March 2009. GFCM Report. No. 33. Rome, FAO. 2009

FAO-GFCM. (2019). Report of the Working Group on Stock Assessment of Demersal Species (WGSAD)-scientific advisory committee on fisheries (SAC). FAO headquarters, Rome, Italy, 9–14 December 2019. 69 pp.

Fiorentino, F., Ben Hadj Hamida, O., Ben Meriem, S., Gaamour, A., Gristina, M., Jarboui, O., Knittweiss, L., Rjeibi, O., & Ceriola, L. (2013). Synthesis of information on some demersal crustaceans relevant for fisheries target species in the south-Central Mediterranean Sea. GCP/-RER/010/ITA/MSM-TD-32. MedSudMed Technical Documents, 32. 118 pp.

Fiorentino, F., Calleja, D., Colloca, F., Perez, M., Prato, G., Russo, T., Sabatella, R., Scarcella, G., Solidoro, C., & Vrgoč, N. (2019). MANTIS: Marine protected Areas Network Towards Sustainable fisheries in the Central Mediterranean. Final Report. EUROPEAN COMMISSION. Directorate-General for Maritime Affairs and Fisheries. Directorate D — Fisheries policy Mediterranean and Black Sea. Unit D.1 — Fisheries management Mediterranean and Black Sea. ISBN 978–92–76-17170-6; https://doi.org/10.2771/33931. 333 pp. (https://op.europa.eu/fr/publication-detail/-/publication/11251e93-f17e-11ea-991b-01aa75ed71a1/language-en/format-PDF/source-153081078

Fiorentino, F., Massutí, E., Tinti, F., Somarakis, S., Garofalo, G., Russo, T., Facchini, M.T., Carbonara, P., Kapiris, K., Tugores, P., & Cannas, R. (2014). Stock units: Identification of distinct biological units (stock units) for different fish and shellfish species and among different GFCM-GSA. STOCKMED Deliverable 03: FINAL REPORT. 310 p. September 2014.

Fogarty, M. J., & Botsford, L. W. (2006). Metapopulation dynamics of coastal decapods. In P. Kritzer & P. F. Sale (Eds.), *Marine metapopulations* (Vol. 2006) (pp. 271–319). Academic Press. https://doi.org/10.1016/B978-012088781-1/50011-X

Fortibuoni, T., Bahri, T., Camilleri, M., Garofalo, G., Gristina, M., & Fiorentino, F. (2010). Nursery and spawning areas of deep-water rose shrimp, Parapenaeus longirostris (Decapoda: Penaeidae), in the strait of Sicily. *Journal of Crustacean Biology*, *30*(2), 167–174. https://doi.org/10.1651/09-3167.1

Gačić, M., Borzelli, G. L. E., Civitarese, G., Cardin, V., & Yari, S. (2010). Can internal processes sustain reversals of the ocean upper circulation? The Ionian Sea example, Geophys. *Research Letters*, *37*(9), L09608. https://doi.org/10.1029/2010GL043216

Gačić, M., Civitarese, G., Kovačević, V., Ursella, L., Bensi, M., Menna, M., Cardin, V., Poulain, P.-M., Cosoli, S., Notarstefano, G., & Pizzi, C. (2014). Extreme winter 2012 in The Adriatic: An example of climatic effect on the BiOS rhythm. *Ocean Science*, *10*(3), 513–522.

Gargano, F., Garofalo, G., & Fiorentino, F. (2017). Exploring connectivity between spawning and nursery areas of Mullus barbatus (L., 1758) in the Mediterranean through a dispersal model. *Fisheries Oceanography*, *26*(4), 476–297. https://doi.org/10.1111/fog.12210

Garofalo, G., Fezzani, S., Gargano, F., Milisenda, G., Ben Abdallah, O., Ben Hadj Hamida, N., Jarboui3, O., Chemmam-Abdelkader, B., Khoufi, W., Micallef, R., Mifsud, R., Gancitano, S., Rizzo, P., Zgozi, S., Ceriola, L., Arneri, E., & Fiorentino, F. (2018). Predictive distribution models of European hake in the south-Central Mediterranean Sea. *Hydrobiologia*, *821*(1), 153–172. https://doi.org/10.1007/s10750-017-3338-5

Garofalo, G., Fortibuoni, T., Gristina, M., Sinopoli, M., & Fiorentino, F. (2011). Persistence and co-occurrence of demersal nurseries in the strait of Sicily (Central Mediterranean): Implications for fishery management. *Journal of Sea Research*, *66*(1), 29–38. https://doi.org/10.1016/j.seares.2011.04.008

Getis, A., & Ord, J. K. (1992). The analysis of spatial association by use of distance statistics. *Geographical Analysis*, *24*(3), 189–206. https://doi.org/10.1111/j.1538-4632.1992.tb00261.x

Heldt, H. (1938). La reproduction chez les Crustacés décapodes de la famille des Pénéides. *Institut Océanographique*, *18*, 1–206.

Hidalgo, M., Rossi, V., Monroy, P., Ser-Giacomi, E., Hernández-García, E., Guijarro, B., Massutí, E., Alemany, F., Jadaud, A., Perez, J. L., & Reglero, P. (2019). Accounting for ocean connectivity and hydroclimate in fish recruitment fluctuations within transboundary metapopulations. *Ecological Applications*, *29*(5), e01913. https://doi.org/10.1002/eap.1913

Hilborn, R., Quinn, T. P., Schindler, D. E., & Rogers, D. E. (2003). Biocomplexity and fisheries sustainability. *Proceedings of the National Academy of Sciences*, *100*(11), 6564–6568. https://doi.org/10.1073/pnas.1037274100

Hinata, H., Ohno, K., Sagawa, N., Kataoka, T., & Takeoka, H. (2020). Numerical modeling of the beach process of marine plastics: 2. A diagnostic approach with onshore-offshore advection-diffusion equations for buoyant plastics. *Marine Pollution Bulletin*, *160*, 111548. https://doi.org/10.1016/j.marpolbul.2020.111548

Huret, M., Runge, J. A., Chen, C., Cowles, G., Xu, Q., & Pringle, J. M. (2007). Dispersal modeling of fish early life stages: Sensitivity with application to Atlantic cod in the western gulf of Maine. *Marine Ecology Progress Series*, *347*, 261–274. https://doi.org/10.3354/meps06983

Kerr, L. A., & Goethel, D. R. (2014). Simulation modelling as a tool for synthesis of stock identification information. In S. X. Cadrin, L. A. Kerr, & S. Mariani (Eds.), *Stock identification methods: Applications in fishery science* (2nd ed.) (pp. 501–533). Elsevier Science and Technology. https://doi.org/10.1016/B978-0-12-397003-9.00021-7

Kerr, L. A., Hintzen, N. T., Cadrin, S. X., Clausen, L., Worsøe Dickey-Collas, M., Goethel, D. R., Hatfield, E. M. C., Kritzer, J. P., & Nash, R. D. M. (2017). Lessons learned from practical approaches to reconcile mismatches between biological population structure and stock units of marine fish. *ICES Journal of Marine Science*, *74*(6), 1708–1722. https://doi.org/10.1093/icesjms/fsw188

Kritzer, J. P., & Liu, O. R. (2014). Fishery management strategies for addressing complex spatial structure in Marine Fish stocks. In S. X. Cadrin, L. A. Kerr, & S. Mariani (Eds.), *Stock identification methods: Applications in fishery science* (second ed.) (pp. 29–58). Elsevier. https://doi.org/10.1016/B978-0-12-397003-9.00003-5

Lacorata, G., Palatella, L., & Santoleri, R. (2014). Lagrangian predictability characteristics of an ocean model. *Journal of Geophysical Research, Oceans*, *119*, 8029–8038. https://doi.org/10.1002/2014JC010313

Lambert, J. D., & Lambert, D. (1991). *Numerical methods for ordinary differential systems: The initial value problem*. Wiley.

Legrand, T., Di Franco, A., Ser-Giacomi, E., Caló, A., & Rossi, V. (2019). A multidisciplinary analytical framework to delineate spawning areas and quantify larval dispersal in coastal fish. *Marine Environmental Research*, *151*, 104761. https://doi.org/10.1016/j.marenvres.2019.104761

Levi, D., Andreoli, M. G., Bonanno, A., Fiorentino, F., Garofalo, G., Mazzola, S., Norrito, G., Patti, B., Pernice, G., Ragonese, S., Giusto, G. B., & Rizzo, P. (2003). Embedding Sea-surface temperature anomalies in the stock–recruitment relationship of red mullet (Mullus barbatus L. 1758) in the strait of Sicily. *Scientia Marina*, *67*(1), 259–268. https://doi.org/10.3989/scimar.2003.67s1259

Levi, D., Andreoli, M. G., & Giusto, R. M. (1995). First assessment of the rose shrimp, *Parapenaeus longirostris* (Lucas 1846), in the Central Mediterranean. *Fisheries Research*, *21*, 375–393. https://doi.org/10.1016/0165-7836(94)00298-B

Liu, F., Mikolajewicz, U., & Six, K. D. (2021). Drivers of the decadal variability of the north Ionian gyre upper layer circulation during 1910–2010: A regional modelling study. *Climate Dynamics*, 1–13. https://doi.org/10.1007/s00382-021-05714-y

Liubartseva, S., Coppini, G., Lecci, R., & Clementi, E. (2018). Tracking plastics in the Mediterranean: 2D Lagrangian model. *Marine Pollution Bulletin*, *129*(1), 151–162. https://doi.org/10.1016/j.marpolbul.2018.02.019

Lo Brutto, S., Maggio, T., & Arculeo, M. (2013). Isolation by distance (IBD) signals in the deep-water rose shrimp *Parapenaeus longirostris* (Lucas, 1846) (Decapoda, Panaeidae) in the Mediterranean Sea. *Marine Environmental Research*, *90*, 1–8. https://doi.org/10.1016/j.marenvres.2013.05.006

Mansui, J., Molcard, A., & Ourmieres, Y. (2015). Modelling the transport and accumulation of floating marine debris in the Mediterranean basin. *Marine Pollution Bulletin*, *91*(1), 249–257. https://doi.org/10.1016/j.marpolbul.2014.11.037

Melaku Canu, D., Laurent, C., Morello, E. B., Querin, S., Scarcella, G., Vrgoc, N., Froglia, C., Angelini, S., & Solidoro, C. (2020). Nephrops norvegicus in the Adriatic Sea: Connectivity modeling, essential fish habitats, and management area network. *Fisheries Oceanography*, *00*(2020), 1–17.

Nicolle, A., Garreau, P., & Liorzou, B. (2009). Modelling for anchovy recruitment studies in the Gulf of lions (Western Mediterranean Sea). *Ocean Dynamics*, *59*(2009), 953–968. https://doi.org/10.1007/s10236-009-0221-6

Oddo, P., Adani, M., Pinardi, N., Fratianni, C., Tonani, M., & Pettenuzzo, D. (2009). A nested Atlantic-Mediterranean Sea general circulation model for operational forecasting. *Ocean Science*, *5*, 461–473. https://doi.org/10.5194/os-5-461-2009

Onink, V., Jongedijk, C. E., Hoffman, M. J., van Sebille, E., & Laufkötter, C. (2021). Global simulations of marine plastic transport show plastic trapping in coastal zones. *Environmental Research Letters*, *16*, 064053. https://doi.org/10.1088/1748-9326/abecbd

Ospina-Alvarez, A., Parada, C., & Palomera, I. (2012). Vertical migration effects on the dispersion and recruitment of European anchovy larvae: From spawning to nursery areas. *Ecological Modelling*, *231*, 65–79. https://doi.org/10.1016/j.ecolmodel.2012.02.001

Ottersen, G., Stige, L. C., Durant, J. M., Chan, K. S., Rouyer, T. A., Drinkwater, K. F., & Stenseth, N. C. (2013). Temporal shifts in recruitment dynamics of North Atlantic fish stocks: Effects of spawning stock and temperature. *Marine Ecology Progress Series*, *480*, 205–225. https://doi.org/10.3354/meps10249

Palatella, L., Bignami, F., Falcini, F., Lacorata, G., Lanotte, A. S., & Santoleri, R. (2014). Lagrangian simulations and interannual variability of anchovy egg and larva dispersal in the Sicily Channel. *Journal of Geophysical Research: Oceans*, *119*, 1306–1323. https://doi.org/10.1002/2013JC009384

Patti, B., Torri, M., & Cuttitta, A. (2020). General surface circulation controls the interannual fluctuations of anchovy stock biomass in the Central Mediterranean Sea. *Scientific Reports*, *10*, 1554. https://doi.org/10.1038/s41598-020-58028-0

Piccioni, A., Gabriele, M., Salusti, E., & Zambianchi, E. (1988). Wind-induced upwellings off the southern coast of Sicily. *Oceanologica Acta*, *11*(4), 309–314.

Pinardi, N., & Masetti, E. (2000). Variability of the large scale circulation of the Mediterranean Sea froma observations and modeling: A review. *Palaeogeography Palaeoclimatology Palaeoecology*, *158*(3–4), 153–173. https://doi.org/10.1016/S0031-0182(00)00048-1

Pinardi, N., Zavatarelli, M., Adani, M., Coppini, G., Fratianni, C., Oddo, P., Simoncelli, S., Tonani, M., Lyubartsev, V., Dobricic, S., & Bonaduce, A. (2015). Mediterranean Sea large-scale low-frequency ocean variability and water mass formation rates from 1987 to 2007: A retrospective analysis. *Progress in Oceanography*, *132*, 318–332. https://doi.org/10.1016/j.pocean.2013.11.003

Pires, R. F. T., Peliz, A., & dos Santos, A. (2021). Into the deep – Dispersal models for deep-water decapod shrimp larvae: The case of *Parapenaeus longirostris*. *Progress in Oceanography*, *194*, 102568. https://doi.org/10.1016/j.pocean.2021.102568

Politou, C. Y., Tserpes, G., & Dokos, J. (2008). Identification of deep-water pink shrimp abundance distribution patterns and nursery grounds in the eastern Mediterranean by means of generalized additive modelling. *Hydrobiologia*, *612*, 99–107. https://doi.org/10.1007/s10750-008-9488-8

Quattrocchi, G., Sinerchia, M., Colloca, F., Fiorentino, F., Garofalo, G., & Cucco, A. (2019). Hydrodynamic controls on connectivity of the high commercial value shrimp *Parapenaeus longirostris* (Lucas, 1846) in the Mediterranean Sea. *Scientific Reports*, *9*, 16935. https://doi.org/10.1038/s41598-019-53245-8

Russo, T., D'Andrea, L., Franceschini, S., Accadia, P., Cucco, A., Garofalo, G., Gristina, M., Parisi, A., Quattrocchi, G., Sabatella, R. F., Sinerchia, M., Canu, D. M., Cataudella, S., & Fiorentino, F. (2019). Simulating the effects of alternative management measures of trawl fisheries in the Central Mediterranean Sea: Application of a multi-species bio-economic modeling approach. *Frontiers in Marine Science*, *6*, 542. https://doi.org/10.3389/fmars.2019.00542

Sobrino, I., Silva, C., Sbrana, M., & Kapiris, K. (2005). A review of the biology and fisheries of the deep water rose shrimp, *Parapenaeus longirostris*, in European Atlantic and Mediterranean waters (Decapoda, Dendrobranchiata, Penaeidae). *Crustaceana*, *78*(10), 1153–1184. https://doi.org/10.1163/156854005775903564

Sorgente, R., Drago, A., & Ribotti, A. (2003). Seasonal variability in the Central Mediterranean Sea circulation. *Annales de Geophysique*, *21*, 299–322. https://doi.org/10.5194/angeo-21-299-2003

Sorgente, R., Olita, A., Oddo, P., Fazioli, L., & Ribotti, A. (2011). Numerical simulation and decomposition of kinetic energy in the Central Mediterranean: Insight on mesoscale circulation and energy conservation. *Ocean Science*, *7*(4), 503–519. https://doi.org/10.5194/os-7-503-2011

Tonani, M., Pinardi, N., Pistoia, J., Dobricic, S., Pensieri, S., de Alfonso, M., & Nittis, K. (2009). Mediterranean forecasting system: Forecast and analysis assessment through skill scores. *Ocean Science*, *5*(4), 649–660. https://doi.org/10.5194/os-5-649-2009

Torrado, H., Mourre, B., Raventos, N., Carreras, C., Tintoré, J., Pascual, M., & Macpherson, E. (2021). Impact of individual early life traits in larval dispersal: A multispecies approach using backtracking models. *Progress in Oceanography*, *192*, 102518. https://doi.org/10.1016/j.pocean.2021.102518

Torres, A. P., Dos Santos, A., Alemany, F., & Massutí, E. (2013). Larval stages of crustacean species of interest for conservation and fishing exploitation in the western Mediterranean. *Scientia Marina*, *77*(1), 149–160. https://doi.org/10.3989/scimar.03749.26D

Torri, M., Corrado, R., Falcini, F., Cuttitta, A., Palatella, L., Lacorata, G., Patti, B., Arculeo, M., Mifsud, R., Mazzola, S., & Santoleri, R. (2018). Planktonic stages of small pelagic fishes (Sardinella aurita and Engraulis encrasicolus) in the Central Mediterranean Sea: The key role of physical forcings and implications for fisheries management. *Progress in Oceanography*, *162*, 25–39. https://doi.org/10.1016/j.pocean.2018.02.009

Werner, F., Cowen, R. K., & Paris, C. B. (2007). Coupled biological and physical models: Present capabilities and necessary developments for future studies of population connectivity. *Oceanography*, *20*(3), 54–69. https://doi.org/10.5670/oceanog.2007.29

Clavel-Henry. M., Solé. J., Bahamon. N., Carretón. M., & Company. J. B. (2021). Larval transport of Aristeus antennatus shrimp (Crustacea: Decapoda: Dendrobranchiata: Aristeidae) near the Palamós submarine canyon (NW Mediterranean Sea) linked to the North Balearic Front. *Progress in Oceanography*, *192*, 102515. https://doi.org/10.1016/j.pocean.2021.102515

SUPPORTING INFORMATION

Additional supporting information may be found in the online version of the article at the publisher's website.

How to cite this article: Gargano, F., Garofalo, G., Quattrocchi, F., & Fiorentino, F. (2022). Where do recruits come from? Backward Lagrangian simulation for the deep water rose shrimps in the Central Mediterranean Sea. *Fisheries Oceanography*, 1–15. https://doi.org/10.1111/fog.12582